Available online at www.sciencedirect.com

ScienceDirect

Procedia Engineering 10 (2011) 2663–2671

Engineering Procedia

ICM11

Effect of Specimen Size in the Kolsky Bar

Srinivasan Arjun Tekalur[a,*], Oishik Sen[a]

[a]*Michigan State University, 2727 Alliance Drive, Lansing, MI-48910, USA*

Abstract

In the current investigation, the effect of specimen size in a Kolsky Bar experiment has been analyzed. By a series of experiments, it has been shown that while determining the dynamic stress-strain relationship of a material using a non-cylindrical specimen, a judicious choice of specimen dimensions helps overcome size effects and estimates the flow stress of the material with reasonable accuracy. Similarly a dependence of the strength of the joint on the overlap area has been observed while finding the dynamic strength of an adhesive-bonded single-lap joint.

Keywords: Size effects; non-cylindrical specimens; slenderness ratio; equilibrium time; single-lap joints; overlap area; Kolsky Bar

1. Introduction

A Kolsky Bar consists of two long cylindrical bars, called the incidence and transmission bars, and a small cylindrical specimen of the material of interest sandwiched between the two bars. A projectile of the same material and same cross-sectional area as the incidence bar is launched at a known velocity towards the incidence bar. This generates a travelling wave in the latter, which subsequently impinges on the specimen, and due to mismatch of mechanical impedance between the bars and the sample, a part of the wave is reflected back as a tensile wave into the incidence bar and a part of it travels forth into the transmission bar as a compressive wave. From the theories of elastodynamics, the following relations can be established **[1]**.

$$\sigma_s(t) = \frac{A_0 E_0 \varepsilon_t(t)}{A_s} \tag{1}$$

$$\dot{\varepsilon}_s = -\frac{2c_0 \varepsilon_r(t)}{L_s} \tag{2}$$

$$\varepsilon_s(t) = \int_0^t \dot{\varepsilon}_s(\tau) d\tau \tag{3}$$

* Corresponding author. Tel.:+01-517-884-1608; fax:+1-517-884-1601.
E-mail address: tsarjun@egr.msu.edu

Selection and peer-review under responsibility of ICM11 doi:10.1016/j.proeng.2011.04.444

where σ_s and ε_s are the nominal stress and strain in the specimen respectively, A_s and L_s are the area of cross-section and length of the specimen respectively, A_0 , E_0 and c_0 are the area of cross-section, Young's modulus and velocity of propagation of a sound wave in the incidence/ transmission bar respectively and ε_r and ε_t refer to the reflected wave and transmitted wave measured by strain-gages placed at the mid-section of the incidence bar and transmission bar respectively.

The calculations presented in the previous section pertain to the determination of dynamic stress-strain relationship of a material of interest. Traditionally, this category of experiments proceeds with a cylindrical sample and the optimal aspect ratio of the specimen to be adopted has been widely researched and established [2,3,4]. This critical slenderness ratio is imperative to ensure that the results obtained from a Kolsky Bar experiment reflect the desired material properties, independent of both the structural properties (such as the diameter and length of the sample) and as far as possible, the boundary-conditions of the problem (such as the effect of friction). Instances of non-cylindrical specimens can be found in relatively recent research works [5-8]. The deviation from cylindrical to non-cylindrical specimens is a matter of convenience for two reasons. Firstly, some types of materials being either extra-soft (such as muscles [9]**)** or highly brittle such as bones [10] are difficult to be machined into a cylindrical shape. Secondly, a non-cylindrical specimen with at least one-flat face renders the specimen amenable to a two-dimensional image correlation analysis for the study of specimen strain, as opposed to a cylindrical specimen, which requires at least two high-speed cameras for it to be amenable to an image correlation analysis. Examples of combining the Kolsky Bar experimental technique with image correlation algorithm can be found in a number of works in this field [11-14]. Studies concentrating on shape-effects when deviating from cylindrical to non-cylindrical specimen has been carried out [5,15]. However, to the best of the authors' knowledge, no attempts have been made to establish a design criterion (i.e. a slenderness ratio) while selecting a non-cylindrical specimen. The focus of the current paper is to propose a characteristic cross-sectional dimension of a non-cylindrical specimen and subsequently propose a suitable slenderness ratio of a non-cylindrical specimen that will help to overcome size and shape effects.

A second category of experiment concerns the determination of the dynamic strength of adhesive-bonded single lap joints using a Kolsky Bar. The specification for the determination of the dynamic strength of adhesive joints, such as ASTM D 905-03 [16] and ISO EN 11343 adhesives [17], involve relatively lower impact velocities and can unfortunately, give only a comparative estimate of the adhesive strength [18]. The determination of dynamic strength of mechanical joints (adhesive-bonded lap joints/butt joints) using a Kolsky Bar has been carried out recently [19-24]. For the case of determination of the strength of an adhesive-bonded single lap joint, a split-cylinder sample is often used [19,25]. This comprises a cylinder, cut along the longitudinal axis of symmetry and bonded with a thin layer of adhesive, which in this case is a two-part epoxy adhesive (Loctite Fixmaster® 99393). There is an additional flange on each of the cylinders to enable centering and minimize associated peel stress. A small gap is left at either ends of the overlap area to ensure load transfer occurs through the adhesive layer alone. The specimen is then sandwiched between the incidence and transmission bars, and the travelling compressive wave generated in the incidence bar by impacting it with a projectile impinges upon the joint. A part of this passes on as a compressive wave into the transmission bar while a part is reflected back into the incidence bar. If it be assumed that the stiffness of the joint is only due to the presence of the adhesive layer, then the peak of the transmitted pulse is a measure of the maximum load the joint can withstand. The procedure for calculation of the joint-strength, loading rate can be found in literature [19]. A research by Srivastava *et. al.*[25] shows that the strength of the joints using a Kolsky Bar is effected by the lap length and out-of-plane thickness of the joint, i.e. the strength of the adhesive joint, as calculated in a Kolsky Bar experiment is dependent on the specimen size. The aim of this work is to show that such a size effect is only *prima facie* and occurs due to the fact that the Kolsky Bar Experiments enables estimation of the average strength of the joint.

2. Size-effects in Experiments on Material Characterization

As discussed in the previous section, for accurate determination of the dynamic stress-strain of a material in a Kolsky bar, the selection of an appropriate specimen slenderness ratio of a specimen is crucial to avoid size-effects. The selection of an appropriate slenderness ratio is generally restricted by three conditions [26].

- Effect of interfacial friction is negligible. To implement this condition, a procedure as developed by Hartley [27] has been adopted.
- The effect of axial inertia in the specimen is negligible. This means that the force on the specimen is constant throughout its length and there is no wave-propagation effect. It can be shown [28-31] that smaller the specimen length, more quickly is this condition met.
- The effect of radial inertia in the specimen is negligibly small.

Radial inertia refers to the condition that when a sample is acted upon by a compressive force, due to Poisson's effect, the sample tries to expand radially. It can be shown that this expansion is accompanied by a non-uniform distribution of stresses along the cross-section of the sample, but the downstream strain-gages on the transmission bar only predicts the average strain across the samples cross-section. Attempts to measure the average sample stress, taking into account the effect of radial inertia have been carried out by many researchers [1, 2, 32-37]. While this is limited to cylindrical specimens, such derivations show that the diameter of the sample is the characteristic cross-sectional dimension of a sample in a Kolsky Bar experiment. This inference is quite trivial in case of a cylindrical specimen. However, on performing similar derivation for a non-cylindrical specimen it can be seen that this helps one to arise at a characteristic cross-sectional dimension for a non-cylindrical specimen. Here, we adopt a procedure similar to Samanta [32] to estimate the extra stress-components arising due to inertia. While the derivation of Samanta [32] and other researchers [1, 2, 31-37] is based on the well-known conservation of mechanical energy principle in the sample, the works stems from the fact that the specimen is hypothesized to behave as an axisymmetric one, with only two independent components of velocity, namely the velocity in the radial direction and the velocity along the length of the specimen. In addition to this, each component of velocity is also assumed, typically, to depend only the radial distance of the point of interest from the origin (selected at the center of the circular cross-section of the specimen) and the longitudinal length of the point of interest. This works well for cylindrical specimens, however, when the specimen is non-cylindrical (but prismatic), it is necessary to change from cylindrical polar coordinates to rectangular Cartesian coordinates. The detailed derivation is not presented here, for the purpose of brevity, and only the key points are summarized here. On changing the coordinate system to a rectangular Cartesian one, it can be shown that there are three independent components of velocities in the specimen, and these are related to one another if it is assumed that the material behaves as an incompressible one. On substituting these components of velocities into the principle of conservation of mechanical energy, in a manner similar to that of Samanta [32], it can be shown that $\sqrt{J/A}$ forms the characteristic cross-sectional dimension of a specimen of an arbitrary cross-section, where J is the polar moment of inertia of the cross-section of the specimen and A is the area of the specimen's cross-section. This is due to the fact that the in net resultant conservation of energy equation in the Cartesian coordinates $\sqrt{J/A}$ replaces the terms involving the diameter in the model for a specimen with a cylindrical cross-section.

For a cylinder of length l and diameter d, J/A is equal to $d^2/8$ and for a cylinder and the critical slenderness ratio to avoid size-effects is established as [3]

$$0.5 \le \frac{l}{d} \le 1 \tag{4}$$

The hypothesis of the current investigation is that the dynamic stress-strain curve of a specimen of any cross-section with a slenderness ratio given by

$$1.4 \le \frac{l}{\sqrt{\frac{J}{A}}} \le 2.8 \tag{5}$$

should be independent of the specimen size, provided interfacial friction is properly reduced. To verify this, experiments were performed with aluminium samples (Al 6061 T6) of hexagonal and rectangular cross-sections at a nearly constant strain-rate (1100-1300/s). The advantage of aluminium specimen is that this being a metallic specimen, wave-propagation effects can be generally neglected for most of the duration of the experiment and the extra stresses induced due to radial inertia is negligibly small, compared to the flow-stress of the material of the specimen. Also, interfacial friction being material

Table 1: Details of the Specimens adopted for an experiment on material characterization

Cross-section of the Specimen	Length of the Specimen	$\sqrt{J/A}$	Nomenclature
Hexagon Edge Size: 6 mm	5.5 mm	1.4	Hexshort
	8 mm	2	Hexlong
Rectangle Edge Size: 6.5 mm x 12.7 mm	6 mm	1.5	Recshort
	8 mm	1.9	Reclong
Circle Diameter: 12.7 mm	6.4 mm	1.4	Circshort
	9 mm	2	Circlong

specific, can be reduced to a large extent for aluminium specimen following the recommendation of Hartley [27]. Table 1 shows the details of the specimens adopted in the current investigation.

Figure 1(a) through 1(c) shows the stress-strain curve at nearly same strain strain-rates for specimens of a given cross-sections. It can be seen that for a given cross-section if the specimen length is changed, then there is no effect of specimen length on the dynamic stress-strain curve of the specimen, provided the length of the specimen is governed by (9). Furthermore, from figure 1(d), it can also be seen that the shape of the specimen does not drastically affect the stress-strain curve of the material, and the flow stress as estimated by non-cylindrical specimen is within 10% of that estimated by cylindrical specimen. Therefore, experiments on determination of the dynamic stress-strain properties of a material using a Kolsky Bar are size-independent, provided the size of the specimen is carefully designed.

3. Size Effects in Experiments on Structural Properties: Adhesive Lap Joints

For the determination of the dynamic strength of single lap joints, Split Cylinder Samples are adopted. The material is High Yield Strength Aluminum (Alloy 7075), which is the same for the incidence/transmission bars. The bonding faces of the samples were first polished using a 600 SiC Grit,

followed by a 1300 SiC Grit. The surface was then cleaned with a phosphoric acid surface cleaner, followed by neutralizing with ammonia water. The surfaces were then bonded using a thin layer of Loctite Fixmaster® High Performance Epoxy (99393), a two-part epoxy adhesive with a mix-ratio of 1:1. The adhesive thickness was maintained to nearly 0.5 mm in all cases. Two different cases of different overlap area were investigated. Table 2 shows the details of the sample used in the current investigation.

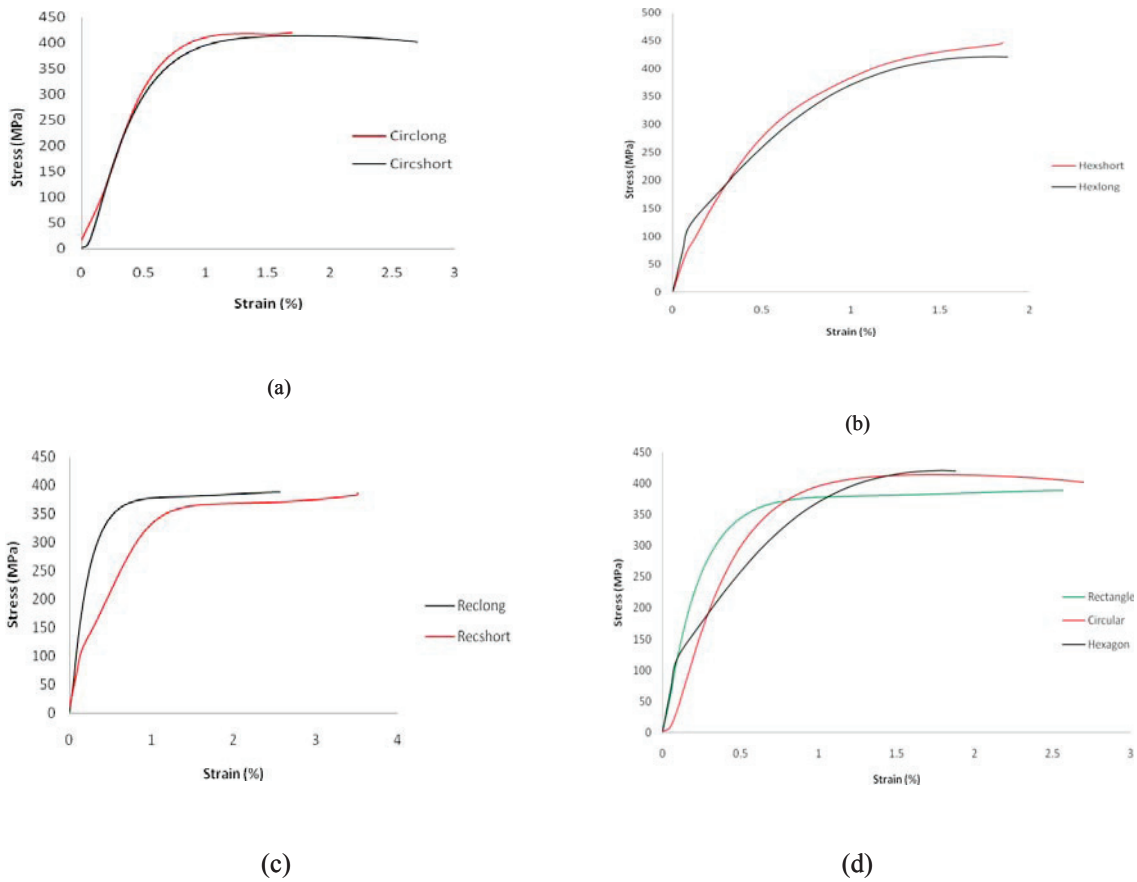

Figure 1. Effect of Change of Specimen Length (a) Circle (b) Hexagon (c) Rectangle (d) All Specimens

In addition to dynamic experiments, quasi-static experiments were also performed using an MTS-810 Material Testing System with a cross-head speed of 0.5mm/s. Figure 2 shows the results from the experiments on the dynamic strength of adhesive lap joints. It can be seen from figure 2, that for a given area of overlap, the joint strength increases with the increase of loading-rate, however, for a given loading rate, the joint-strength decreases with an increase in overlap area. Therefore, the dynamic strength of adhesive-bonded single lap joint is significantly dependent on the overlap area.

In order to explore further into the drastic effect of overlap area on the dynamic strength of the joints, a mathematical model for the adhesive joint was developed. The development of mathematical model for adhesive-bonded lap joints have been done extensively in literature [38-43], however, studies have been

Table 2: Specimens adopted in the current investigation

Name	Overlap Length (x_l) (mm)	Diameter *(d)*(mm)	Overlap Area (A), (mm^2)
1	15	15.9	238.5
2	15	12.7	190.5

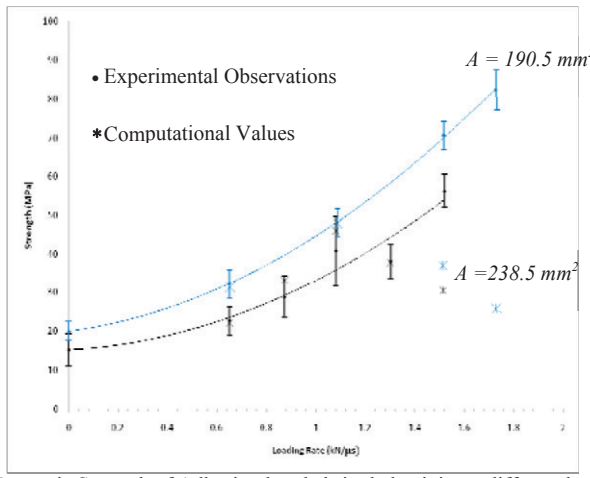

Figure 2. Dynamic Strength of Adhesive-bonded single lap joint at different loading rate

restricted to the development of governing equations for quasi-static cases only. In the current investigation, following the key steps of Osnes *et. al.* [43], an attempt has been made to develop a governing equation for the case of an adhesive joint, subjected to dynamic loading. The development rests on the classical "shear-lag" theory and takes into account the effect of strain-acceleration and out-of-plane adhesive thickness. As the derivation follows from that of Osnes *et. al.* [43] for the purpose of brevity, only the final result is presented in the current derivation. It can be shown that under the assumptions of the classical "shear-lag" theory, the following equation governs the shear strain (γ_a) in the adhesive layer.

$$\frac{\partial^2 \gamma_a}{\partial x^2} - \frac{1}{c^2}\frac{\partial^2 \gamma_a}{\partial t^2} = \frac{1}{\alpha}\gamma_a \tag{6}$$

where α is a parameter given by

$$\frac{1}{\alpha} = \frac{72 G_a G}{E\left(9G\pi r t_a - 4r^2 G_a\right)} \tag{7}$$

Here, G and E are the Young's modulus and Shear modulus of the adherend with the out-of-plane radius r, and G_a is the Shear modulus of the adhesive layer whose thickness is t_a. The boundary conditions of the problem are those developed by Osnes [43], in which the external forces are taken from the readings of the strain-gages on the incidence bar, after taking into account area mismatch between the incidence bar (complete cylindrical cross-section) and the split-cylinder specimens (which has a semicircular cross-section). Using the weighted residual method, the time-resolved shear strain in the

adhesive layer was calculated from Equation (6). The time taken to reach the peak strain in the transmission bar strain gage was adopted as the time to failure and the strain in the adhesive layer at that time was studied. Figure 3 shows the strain at failure in all the four specimens adopted.

Comparing Figure 3(a) with 3(b) it can be readily concluded that for a given out-of-plane thickness, reduction of the overlap length has very small effect on the peak strain developed in the adhesive, and also the total length of zero strain also remains the same. Thus, the average strain is enhanced by reducing the overlap length. The implication of this is that lower is the overlap area, greater is the average strain. As a Kolsky Bar can only predict the average strength of the joint, hence the results are heavily size-

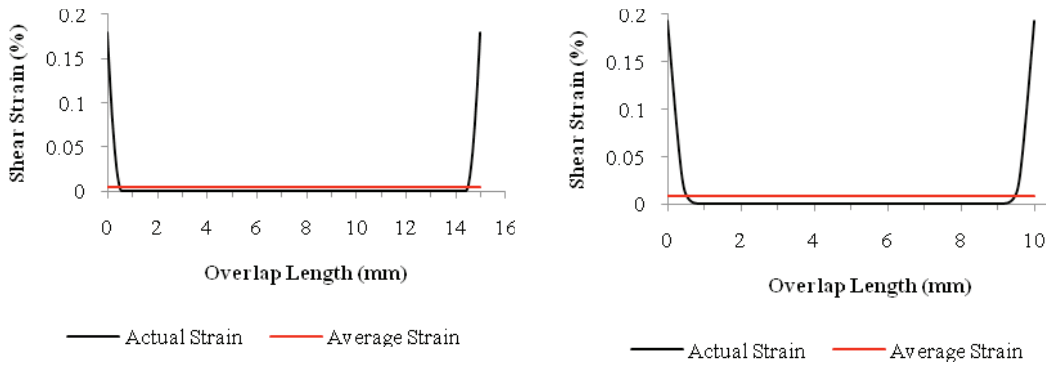

Figure 3. Plot of Shear Strain distribution in the adhesive layer over the overlap length for (a) Sample 1 (b) Sample 2

dependant. From Figure 2, the computational strength can be seen to be agreeable with the experimental average strength over a considerable range of loading rate. The experimental values show disagreement with the computational values at higher loading rates. The cause of this is left as a task for future investigation. It is suspected that the rate-dependant nature of the adhesive can cause this deviation, whereas the current governing differential equation (6) rests on the assumption that the adhesive is rate-independent and linear elastic. Nonetheless, the current model shows reasonably good agreement over a wide range of loading rates, and more importantly provides an explanation for size-effects in Kolsky Bar experiments on determination of dynamic strength of adhesive-bonded single lap joints.

4. Conclusion

The current paper focuses on size effects in a Kolsky Bar experiment. It has been shown that for accurate determination of dynamic stress-strain relationship of a material in a Kolsky bar, size-effects can be minimized by judicious choice of specimen size with proper consideration to friction, equilibrium and radial inertia. For accurate determination of structural strength of an adhesive-bonded single lap joint, it can be seen that there are predominant size effects, i.e. the dynamic strength of the adhesive joints increase with the decrease of overlap area (for a given loading rate). The cause for this has been inspected, and it has been found that this is due to the fact that the Kolsky Bar can predict only the average strength of the joints. But given the theory and experimental validation, we can obtain reasonable strength data using the Kolsky bar setup.

Acknowledgements

The authors express their gratitude to Dr. Arun Shukla, University of Rhode Island, Dr. Gary Cloud, Michigan State University, Dr. V. Parameswaran, Indian Institute of Technology, Kanpur, Dr. S. Hong, Michigan State University, Dr. M.J. Forrestal, Sandia National Laboratories and Dr. W. Chen, Purdue University, for their valuable suggestions and help in course of the research.

References

[1] Kolsky H. An investigation of the mechanical properties of materials at very high rates of loading. *Proc. Phys. Soc.*1949; **B-62:** 676-700

[2] Davies E. D.H., Hunter, S.C. The dynamic compression testing of solids of the method of split Hopkinson pressure bar. *J. Mech. Phys. Solids* 1963; **11**:155–181

[3] Bertholf L.D., Karnes, C.H. Two-dimensional analysis of the split-Hopkinson pressure bar system. *J. Mech. Phys. Solids* 1975; **23**: 1–19

[4] Ramesh KT., High strain rate and impact experiments. In:Sharp WN (ed) *Handbook of experimental solid mechanics,* Springer: 101, Norwell; 2009

[5]Woldesenbet E., Vinson J R. Specimen geometry effects on high-strain-rate testing of graphite/epoxy composites. *AIAA journal* 1999; **37-9:** 1102-1106.

[6]Koerber H., Xavier J., Camanho, P.P. High strain rate characterisation of unidirectional carbon-epoxy IM7-8552 in transverse compression and in-plane shear using digital image correlation. *Mechanics of Materials* 2010; **42**:1004-1019.

[7]Pintado P., Pedraza C., Castillo J.M. del., Benitez F.G. Experimental investigation of the dynamic response of response of graphite-epoxy composite laminates under compression. *Composite Structures* 2001; **53**: 493-497.

[8]Dannemann K.A., Chocron S., Walker J D., Nicholls A E. High strain rate compression testing of RCC materials. *Proceedings of the SEM Annual Conference and Exposition on Experimental and Applied Mechanics 2007* 2007; **2**: 959-960

[9] Song B., Chen W., Ge Y., Weerasooriya T. Dynamic and quasi-static compressive response of porcine muscle. *Journal of Biomechanics* 2007; **40**:2999–3005

[10]Ferreira F., Vaz, M.A., Simoes, J.A. Mechanical properties of bovine cortical bone at high strain rate. *Materials Characterization* 2006; **57**:71–79

[11] Schmidt T., Gilat A, Walker A., Seidt J., Tyson, J. 3D Image correlation studies of geometry and material property effects during split Hopkinson bar experiments. *Society for Experimental Mechanics - 11th International Congress and Exhibition on Experimental and Applied Mechanics 2008* 2008; **3**:1624-1635.

[12] Gilat A., Schmidt T.E., Walker A.L. Full field strain measurement in compression and tensile split Hopkinson bar experiments. *Experimental Mechanics* 2009; **49-2:**291-302.

[13] Schmidt T, Tyson J. 3D and 2D high speed image correlation for dynamic testing. *Society for Experimental Mechanics - SEM Annual Conference and Exposition on Experimental and Applied Mechanics 2009* 2009; **3**:1676-1687.

[14]Siviour C.R. A measurement of wave propagation in the split Hopkinson pressure bar. *Meas. Sci. Technol.* 2009; **20**:1-5.

[15] Pankow M., Attard C., Waas A.M. Specimen size and shape effect in split Hopkinson pressure bar testing. *J. Strain Analysis* 2009; **44**:689-697

[16] ASTM D950-03, Standard test method for impact strength of adhesive bonds. ASTM Int, 2003.

[17]ISO EN 11343 Adhesives- determination of dynamic resistance to cleavage of high-strength adhesive bonds under impact conditions-wedge impact method, 1993.

[18] Adams R.D., Harris J.A. A critical assessment of the block impact test for measuring the impact strength of adhesive bonds. *International Journal of Adhesion and Adhesives* 1996; **16**:61-71

[19] Srivastava V., Shukla A., Parameswaran V. Experimental Evaluation of the Dynamic Shear Strength of Adhesive-Bonded Lap Joints. *Journal of Testing and Evaluation* 2000; **28-6:**438-442

[20] Yokoyama T, Shimizu H. Evaluation of Impact Shear Strength of Adhesive Joints with the Split Hopkinson Bar. *JSME International Journal* 1998; **A-41-4:** 503-509

[21] Yokoyama T., Nakai K. Determination of impact tensile properties of structural epoxy adhesive butt joints using a hat-shaped specimen. *J. Phys. IV France* 2006. **134:**789–795

[22] Adamvalli M., Parameswaran V. Dynamic strength of adhesive lap joints at high temperature. *Int J Adhes &Adhes* 2008; **28**:321–327

[23] Chen X, Li Y. An Experimental Technique on the Dynamic Strength of Adhesively Bonded Single Lap Joints. *Journal of Adhesion Science and Technology* 2010; **24**:291–304

[24] Raykhere S.L., Kumar P, Singh R.K., Parameswaran V. Dynamic shear strength of adhesive joints made of metallic and composite adherents. *Materials and Design* 2010; **31**:2102–2109

[25] Srivastava V., Parameswaran V, Shukla A, Morgan D. Evaluation of the dynamic strength of adhesive joints using split hopkinson pressure bar. *Recent Advances in Experimental Mechanics Special Technical Publication* 2002; 769-780.

[26] Al-Mousawi M.M., Reid S.R., Deans W.F. The use of the split Hopkinson pressure bar techniques in high strain rate materials testing. *Proc. Instn. Mech. Engrs.* 1997; **211-C**:273-292.

[27] Hartley R.S., Cloete T.J., Nurick G.N. An experimental assessment of friction effects in the split Hopkinson pressure bar using the ring compression test. *International Journal of Impact Engineering* 2007; **34**:1705–1728.

[28] Ravichandran G., Subhash G. Critical appraisal of limiting strain rates for compression testing of ceramics in a split Hopkinson pressure bar. *J. Am. Ceram. Soc.* 1994; **77**:263–267

[29] Subhash, G., Ravichandran G. Split Hopkinson Pressure Bar Testing of Ceramics. *Materials Park, OH: ASM International* 2000; 497-504

[30] Wu X.J.,Gorham D.A. Stress equilibrium in the Split Hopkinson Pressure Bar Test. *J. Phys* 1997; **IV**: C391-C396

[31] Yang L.M., Shim V.P.W., An analysis of stress uniformity in split Hopkinson bar test specimens. *International Journal of Impact Engineering 2005; 31:129-150*

[32] Samanta S.K. Dynamic deformation of aluminum and copper at elevated temperatures*. J Mech Phys Solids* 1971*;* **19**:117-135

[33] Gorham D.A. Specimen inertia in high strain-rate compression. *J. Phys. D: Appl. Phys.* 1989; **22**:1888–1893

[34] Gorham D.A. The effect of specimen dimensions on high strain rate compression measurements of copper. *J. Phys. D: Appl. Phys.*1991; **24**:1489–1492

[35] Forrestal M.J., Wright T.W., Chen W. The effect of radial inertia on brittle samples during the split Hopkinson pressure bar test. *International Journal of Impact Engineering* 2007; **34**:405-411

[36] Song B., Ge Y., Chen W.W., Weerasooriya T. Radial Inertia Effects in Kolsky Bar Testing of Extra-soft Specimens. *Experimental Mechanics* 2007; **47**:659-670

[37]Warren T.L., Forrestal M.J. Comments on the Effect of Radial Inertia in the Kolsky Bar Test for an Incompressible Material. *Experimental Mechanics* 2010; **50**:1253–1255

[38] Volkersen O., Die Niektraftverteilung in Zugbeanspruchten mit Konstanten Laschenquerschritten, *Luftfahrtforschung* 1938; **15**: 41–47

[39] Goland M., Reissner E. The stresses in cemented joints. *Journal of Applied Mechanics* 1944; **11**: A17–27.

[40] de Bruyne N.A. The strength of glued joints. *Aircraft Eng.* 1944; **16**:115–118.

[41] Hart-Smith L.J. Adhesive bonded single lap joints. *NASA CR-112236.*1973; 1-114.

[42] Tsai M.Y., Oplinger D.W., Matthews F.L. Improved theoretical solutions for adhesive lap joints. *International Journal of Solids and Structures* 1998; **35-12:**1163–1185.

[43] Osnes H., McGeorge D. Experimental and analytical strength analysis of double-lap joints for marine applications. *Composites: Part B* 2009; **40:**29–40